Supporting information

Highly sensitive and selective SO_2 MOF sensor: The integration of MFM-300 MOF as a sensitive layer on a capacitive interdigitated electrode

by Valeriya Chernikova,[a] Omar Yassine,[b] Osama Shekhah,[a] Mohamed Eddaoudi[a]* and Khaled N. Salama[b]*

a. Functional Materials Design, Discovery and Development Research Group (FMD^3), Advanced Membranes and Porous Materials Center (AMPMC), Division of Physical Sciences and Engineering (PSE), King Abdullah University of Science and Technology (KAUST), Thuwal 23955-6900, Kingdom of Saudi Arabia.

b. Sensors Lab, Electrical Engineering Program, Computer, Electrical and Mathematical Sciences and Electrical Engineering Division, King Abdullah University of Science and Technology, Thuwal 23955-6900, KSA, E-mail: khaled.salama@kaust.edu.sa

* Corresponding authors:

Prof. Mohamed Eddaoudi
Director, KAUST Advanced Membranes & Porous Materials Center
4700 King Abdullah University of Science and Technology
Thuwal 23955-6900, Kingdom of Saudi Arabia
E-mail: mohamed.eddaoudi@kaust.edu.sa

Prof. Khaled Nabil Salama
KAUST Computer, Electrical and Mathematical Sciences and Electrical Engineering Division
4700 King Abdullah University of Science and Technology
Thuwal 23955-6900, Kingdom of Saudi Arabia
E-mail: khaled.salama@kaust.edu.sa

Table of contents:

1. Materials and instrumentation

Powder X-ray diffraction (PXRD) measurements were carried out at room temperature on a PANalyticalX'Pert PRO diffractometer 45kV, 40mA for CuKα (λ = 1.5418 Å), with a scan speed of 1.0° min-1 and a step size of 0.01° in 2θ.

Scanning electron microscope (SEM) characterization was performed using an FEI Quanta 600 field emission SEM (accelerating voltage: 30kV)

Interdigitated electrodes (IDEs) were fabricated on a silicon wafer. A 2 µm oxide layer was thermally grown for electrical isolation. First, a layer of 10 nm Ti and 300 nm Au was deposited via physical vapour deposition (PVD) in an ESC reactive and metal sputter system. Next, photolithography was used to pattern the electrodes. The metal layer was patterned by dry etching using Oxford Instruments PlasmaLab System and the exposed oxide thickness was further verified using Nanospec 6100 Reflectometer to ensure that the metal layer was properly etched. The IDEs were designed with 4µm fingers and 5 µm spaces. Two Au wires and contact pads were patterned to perform the electrical measurements.

Fabrication of MFM-300-MOF thin film: thin films of the MFN-300 MOF were prepared solvothermally. Biphenyl-3,3′,5,5′-tetracarboxylic acid (1.6 mg, 5 µmol), $In(NO_3)_3$ (2.9 mg, 7.5 µmol), DMF (1.7 mL), CH_3CN (0.8 ml) and Nitric acid (0.09 ml of 3.5M solution in DMF) were combined in a 5 mL scintillation vial. After sonication, solution was divided in 3 equal parts and placed in 5 ml vials. Pre-functionalized IDE chips with the MUD SAM (11-Mercapto-1-undecanol) were placed inside vials with freshly prepared solution, sealed, and heated to 85°C over night and then cooled to room temperature. The IDE chip was collected and washed with about 10 mL of anhydrous DMF and immersed in 10 mL of ethanol for 3 days, during which time the ethanol was replaced three times per day.

TG-DSC: The SENSYS TG-DSC instrument (Setaram Instrumentation) was used for heat of adsorption measurement at 25 °C in a flow of nitrogen. The obtained signal is then integrated to give the corresponding amount of heat in Joules. The increments of adsorption were read directly from the TG curve. For TG analysis, the sample was placed in platinum pans and, before experiment, activated by heating in a nitrogen flow at 120 °C for 24 h and brought to the adsorption temperature. Adsorption of water vapor on the sample was performed after flushing the evacuated sample by nitrogen flow for 1 hour.

Gas-sensing tests were performed using the LabVIEW fully automated measurement system. The coated sensor was placed inside the detection chamber and connected to the LCR meter to detect the capacitive change. The samples were first activated under vacuum for one hour; the chamber was later purged with pure nitrogen. Nitrogen gas was used as a carrier gas to dilute the SO_2 to the desired concentration; we worked with a ppb range from 10 to 1000 ppb.

2. Potential MOFs

We compared, to the best of our knowledge, all MOFs reported to have high SO_2 sorption capacity and selectivity for SO_2 over CO_2. Based on this data, our top three candidates were MFM-300 (In), MFM-202-a, and Ni(bdc)(ted)$_{0.5}$. However, the MFM-202-a, with the highest capacity, changes its structure upon desorption, potentially limiting its usefulness as a base material for a sensor. We focused on MFM-300 (In) instead of Ni(bdc)(ted)$_{0.5}$ due to less harsh synthesis conditions, an important factor in the stability of the circuit during deposition. Full data for the MOFs considered are shown in Table S1.

Table S1. Comparison of potential MOFs as a base material for SO_2 sensing

MOF	SO_2 Capacity* mmol/g	CO_2 Capacity* mmol/g.	BET m^2/g	pore volume cc/g	Synthetic conditions		Ref.
					Solvent mixture	Temp./Time	
MFM-300 (In)	8.3	3.6	1071	0.42	DMF, CH_3CN, HNO_3	85°C/12 hours	1
MFM-300 (Al)	7.5	4.4	1370	0.38	Piperazine, H_2O, HNO_3	210°C/3 days	2
MFM-202-a	10.2 (irrev.)	2.5	2220	0.95	DMF, CH_3CN, HNO_3	90°C/1 day	3
$Zn_3[Co(CN)_6]_2$	1.8	1.5	700	0.30	H_2O	RT/1 day	4
$Co_3[Co(CN)_6]_2$	2.5	1.4	712	0.31	H_2O	RT/1 day	4
Mg-MOF-74	8.6	8.5	1640	0.57	H_2O/EtOH	125°C/1 day	5
Ni(bdc)(ted)$_{0.5}$	9.97	2.3	1701	0.74	DMF	120°C/2 days	5

* at 298 K and 1 bar

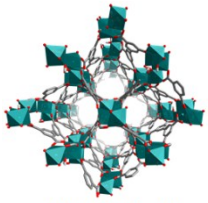
MFM-300 (In,Al)

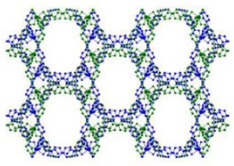
MFM-202-a

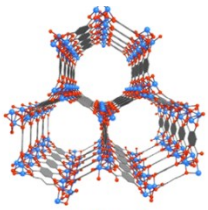
M-MOF-74

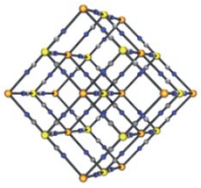
$M_3[Co(CN)_6]_2$

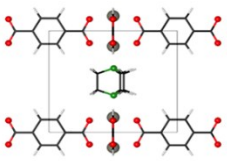
Ni(bdc)(ted)$_{0.5}$

As reported in literature[1,2], the $O^{\delta-}$ of adsorbed SO_2 molecules interact with five hydrogen atoms $H^{\delta+}$- free hydroxyl group on the metal oxide chain and four aromatic C–H groups from the ligand, forming weak cooperative supramolecular interactions. ∠OSO bond angle is around 110-120º. The second site (SO_2) interacts with the first SO_2 through dipole interaction. The authors of [2] are convinced that higher SO_2 uptake compare to CO_2 uptake is attributed to the high dipole moment of SO_2 (1.62 D) compared with 0 D for CO_2. Strong SO_2 dipole-dipole interaction coupled with hydrogen bonding to the framework lead to higher adsorption amount of SO_2 versus CO_2 and other common gases, such as H_2, CH_4, NO_2 at very low concentrations.

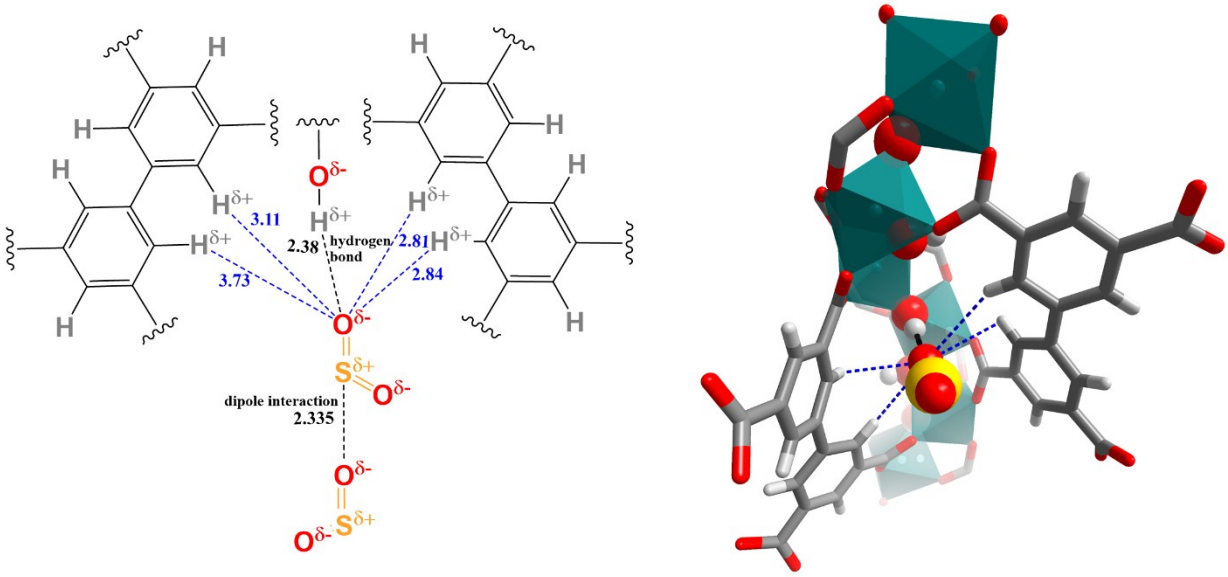

Figure S1. Schematic representation of SO_2 adsorption sites[2].

3. Characterizations

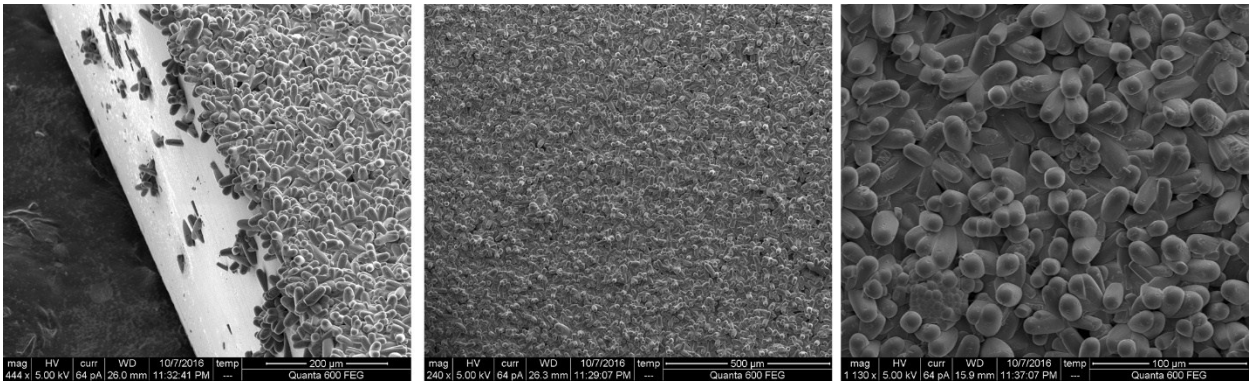

Figure S2. SEM images of MFM-300 (In) on IDE substrate at various magnifications.

To investigate effect of humidity on performance of MFM-300 (In) MOF sensor, water affinity was studied by performing simultaneous thermal gravimetric and calorimetric measurements (TG-DSC) for MFM-300 (In). The enthalpy (DH) of water vapor adsorption (47.2 kJ/mol) was found to be close to the reported value for SO_2[1] adsorption (39.6 kJ/mol). The control experiment was done on CO_2, where enthalpy CO_2 adsorption (27.6 kJ/mol) matches reported value for CO_2[1] adsorption (27.2 kJ/mol), which confirms reliability of the data. Also, enthalpy of water vapor measured for MFM-300 (In) corresponds to the data reported for MFM-300 Scandium analogue (46.8 kJ/mol).[6]

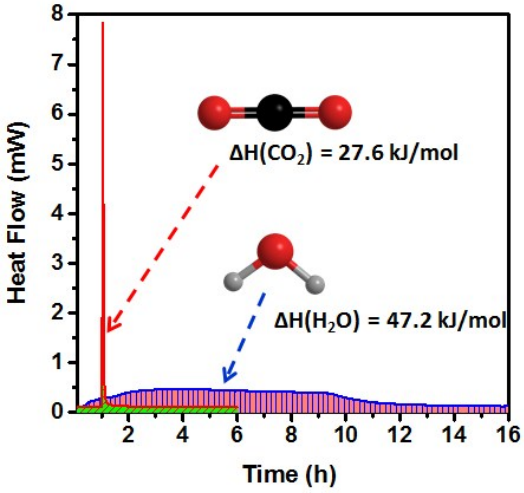

Figure S3. Heat-flow (in mW) for the adsorption of CO_2 (red) and water vapor (blue) on MFM-300 (In) MOF obtained by TG-DSC analysis.

4. Sensor characteristics

4.1 Baseline test

The change in capacitance of the bare chip was tasted in of range of different temperatures (fig. S3) and different SO_2 concentrations (fig. S4). The response difference was less than 0.3% in both cases.

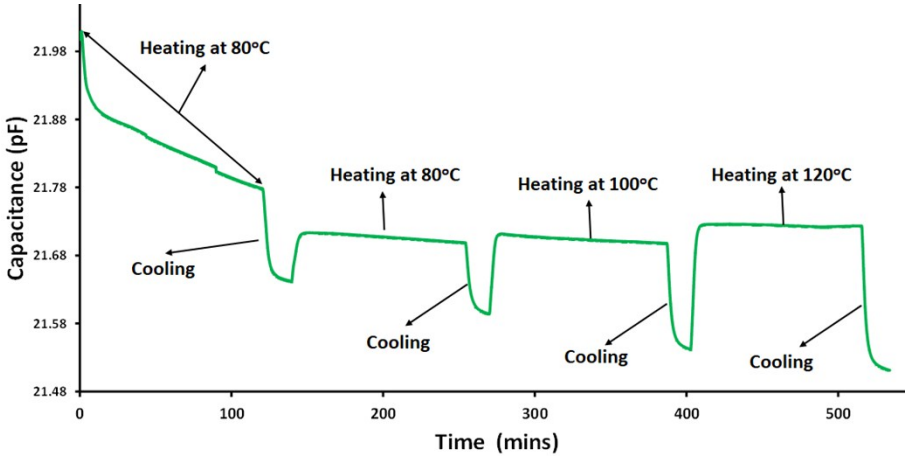

Figure S4. Change in bare chip capacitance at different temperatures

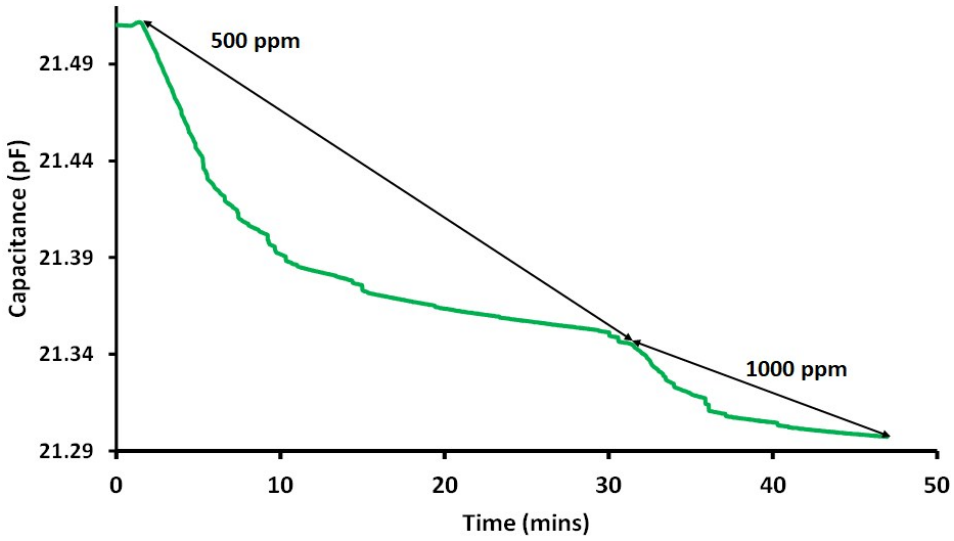

Figure S5. Change in bare chip capacitance in presence of SO_2

4.2 Humidity test of MFM-300 MOF sensor

The sensing of SO_2 is reversible. The Fig.4a was obtained, following the below measurement scheme (Fig. S6).

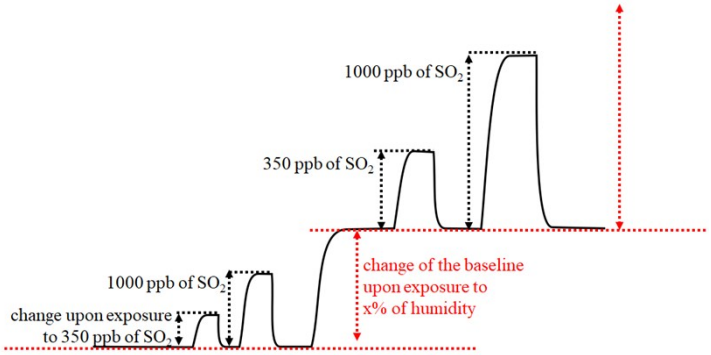

Figure S6. Measurement scheme

The chamber was activated under vacuum and purged with pure nitrogen. The obtained capacitance signal was considered as baseline for dry measurement. The chamber later was exposed to 350 ppb of SO_2 until the capacitance signal rich saturation. The change between 350 ppb and baseline signals was plotted in a graph. After activation (the signal rich baseline value) the chamber was exposed to 1000 ppb of SO_2 until no changes in capacitance were further noticed. The change was plotted (1000 signal – baseline). After activation, the chamber was purged with 5% humidity nitrogen, until the signal was stable. The obtained capacitance signal was considered as baseline for 5% humidity measurement. The protocol was repeated for each level of humidity up to 85%.

The effect of relative humidity on MFN-300 MOF sensor is depicted on Fig. S7.

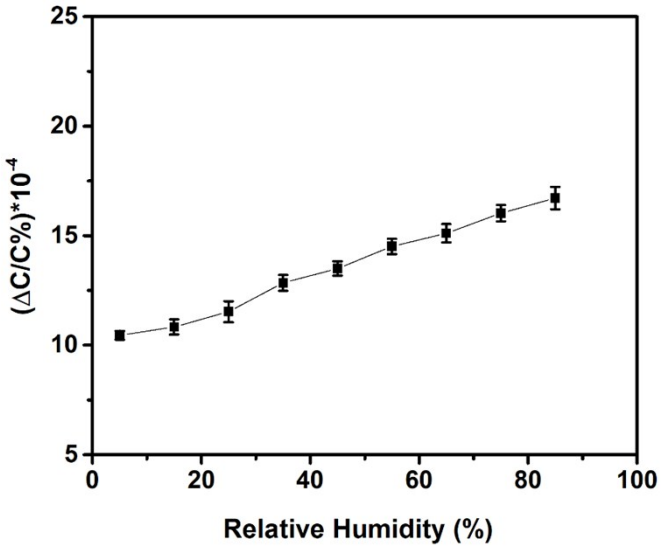

Figure S7. Effects of the relative humidity on the MFM-300 (In) MOF sensor

5. References

1. M. Savage, Y. Cheng, T. L. Easun, J. E. Eyley, S. P. Argent, M. R. Warren, W. Lewis, C. Murray, C. C. Tang, M. D. Frogley, G. Cinque, J. Sun, S. Rudic, R. T. Murden, M. J. Benham, A. N. Fitch, A. J. Blake, A. J. Ramirez-Cuesta, S. Yang and M. Schroder, *Advanced materials*, 2016, **28**, 8705-8711.
2. S. Yang, J. Sun, A. J. Ramirez-Cuesta, S. K. Callear, W. I. David, D. P. Anderson, R. Newby, A. J. Blake, J. E. Parker, C. C. Tang and M. Schroder, *Nat. Chem.*, 2012, **4**, 887-894.
3. S. Yang, L. Liu, J. Sun, K. M. Thomas, A. J. Davies, M. W. George, A. J. Blake, A. H. Hill, A. N. Fitch, C. C. Tang and M. Schroder, *J. Am. Chem. Soc.*, 2013, **135**, 4954-4957.
4. P. K. Thallapally, R. K. Motkuri, C. A. Fernandez, B. P. McGrail and G. S. Behrooz, *Inorg. Chem.*, 2010, **49**, 4909-4915.
5. K. Tan, P. Canepa, Q. Gong, J. Liu, D. H. Johnson, A. Dyevoich, P. K. Thallapally, T. Thonhauser, J. Li and Y. J. Chabal, *Chem. Mater.*, 2013, **25**, 4653-4662.
6. J. R. Álvarez, R. A. Peralta, J. Balmaseda, E. González-Zamora and I. A. Ibarra, *Inorganic Chemistry Frontiers*, 2015, **2**, 1080-1084.